MHCII-independent CD4+ T cells protect injured CNS neurons via IL-4

James T. Walsh, … , Frauke Zipp, Jonathan Kipnis

Research Article

A body of experimental evidence suggests that T cells mediate neuroprotection following CNS injury; however, the antigen specificity of these T cells and how they mediate neuroprotection are unknown. Here, we have provided evidence that T cell–mediated neuroprotection after CNS injury can occur independently of major histocompatibility class II (MHCII) signaling to T cell receptors (TCRs). Using two murine models of CNS injury, we determined that damage-associated molecular mediators that originate from injured CNS tissue induce a population of neuroprotective, IL-4–producing T cells in an antigen-independent fashion. Compared with wild-type mice, IL-4–deficient animals had decreased functional recovery following CNS injury; however, transfer of CD4+ T cells from wild-type mice, but not from IL-4–deficient mice, enhanced neuronal survival. Using a culture-based system, we determined that T cell–derived IL-4 protects and induces recovery of injured neurons by activation of neuronal IL-4 receptors, which potentiated neurotrophin signaling via the AKT and MAPK pathways. Together, these findings demonstrate that damage-associated molecules from the injured CNS induce a neuroprotective T cell response that is independent of MHCII/TCR interactions and is MyD88 dependent. Moreover, our results indicate that IL-4 mediates neuroprotection and recovery of the injured […]

Find the latest version:

https://jci.me/76210/pdf

MHCII-independent CD4+ T cells protect injured CNS neurons via IL-4

James T. Walsh,[1,2,3,4] Sven Hendrix,[5,6] Francesco Boato,[6,7] Igor Smirnov,[1,2] Jingjing Zheng,[1,2,8] John R. Lukens,[1,2,9] Sachin Gadani,[1,2,3,4] Daniel Hechler,[6] Greta Gölz,[6] Karen Rosenberger,[6] Thomas Kammertöns,[10] Johannes Vogt,[6,7] Christina Vogelaar,[7] Volker Siffrin,[11] Ali Radjavi,[1,2,12] Anthony Fernandez-Castaneda,[1,2,3] Alban Gaultier,[1,2,3] Ralf Gold,[13] Thirumala-Devi Kanneganti,[9] Robert Nitsch,[6,7] Frauke Zipp,[11] and Jonathan Kipnis[1,2,3,4,12]

[1]Center for Brain Immunology and Glia, [2]Department of Neuroscience, [3]Graduate Program in Neuroscience, and [4]Medical Scientist Training Program, School of Medicine, University of Virginia, Charlottesville, Virginia, USA. [5]Department of Morphology and BIOMED Institute, Hasselt University, Diepenbeek, Belgium. [6]Institute for Cell Biology and Neurobiology, Center for Anatomy, Charité — Universitätsmedizin Berlin, Berlin, Germany. [7]Institute for Microscopic Anatomy and Neurobiology, Focus Program Translational Neuroscience, University Medical Center, Johannes Gutenberg University Mainz, Mainz, Germany. [8]Institute of Neurosciences, Fourth Military Medical University, Xi'an, China. [9]Department of Immunology, St. Jude Children's Research Hospital, Memphis, Tennessee, USA. [10]Max Delbrück Center for Molecular Medicine, Berlin, Germany. [11]Department of Neurology, Focus Program Translational Neuroscience and Center for Immunotherapy, University Medical Center, Johannes Gutenberg University Mainz, Mainz, Germany. [12]Graduate Program in Microbiology, Immunology and Infectious Diseases, School of Medicine, University of Virginia, Charlottesville, Virginia, USA. [13]Department of Neurology, St. Josef Hospital/Ruhr-University Bochum, Bochum, Germany.

A body of experimental evidence suggests that T cells mediate neuroprotection following CNS injury; however, the antigen specificity of these T cells and how they mediate neuroprotection are unknown. Here, we have provided evidence that T cell–mediated neuroprotection after CNS injury can occur independently of major histocompatibility class II (MHCII) signaling to T cell receptors (TCRs). Using two murine models of CNS injury, we determined that damage-associated molecular mediators that originate from injured CNS tissue induce a population of neuroprotective, IL-4–producing T cells in an antigen-independent fashion. Compared with wild-type mice, IL-4–deficient animals had decreased functional recovery following CNS injury; however, transfer of CD4+ T cells from wild-type mice, but not from IL-4–deficient mice, enhanced neuronal survival. Using a culture-based system, we determined that T cell–derived IL-4 protects and induces recovery of injured neurons by activation of neuronal IL-4 receptors, which potentiated neurotrophin signaling via the AKT and MAPK pathways. Together, these findings demonstrate that damage-associated molecules from the injured CNS induce a neuroprotective T cell response that is independent of MHCII/TCR interactions and is MyD88 dependent. Moreover, our results indicate that IL-4 mediates neuroprotection and recovery of the injured CNS and suggest that strategies to enhance IL-4–producing CD4+ T cells have potential to attenuate axonal damage in the course of CNS injury in trauma, inflammation, or neurodegeneration.

Introduction

Injury to the CNS unleashes a complex series of molecular events underlying both acute and sustained death of neural tissue. Induction of cell death in the CNS triggers a cascade of continuous (secondary) neurodegeneration, resulting in a substantially higher degree of tissue loss than could have been predicted from the severity of the initial damage (1). While the role of T cells in mediating autoimmune neuroinflammation has been studied intensively (2–7), their role in neurodegeneration and neuroprotection is still a matter of debate. T cell inflammation associated with CNS injury was largely viewed as detrimental (8, 9). However, over a decade ago, T cells were shown to play a protective role after injury (10),

challenging the prevailing dogma. Furthermore, based on exogenous administration of autoimmune T cells, it was suggested that the cells mediating such neuroprotection are self reactive (11–13). However, other reports indicated that autoreactive T cells may also be implicated in continuous neurodegeneration after injury (14), leaving open questions, i.e., what makes a T cell protective or pathogenic, what is the antigenic specificity of T cells that respond to injury spontaneously, and what is their mechanism of function in benefitting the injured CNS.

Here, we used two in vivo CNS injury models (optic nerve crush injury and spinal cord contusive injury) to address the impact of T cells both on neuronal survival (after optic nerve crush) and neurological recovery (after spinal cord injury). We show the unexpected observation that neuroprotection mediated by T cells in response to CNS injury does not require MHCII–T cell receptor (MHCII-TCR) interaction and, instead, damage-associated molecular mediators from the injured CNS skew T cells toward IL-4 production in a MyD88-dependent manner. To uncover the underlying molecular mechanisms of this neuroprotective effect, we used in vitro systems to demonstrate that T cell–derived IL-4
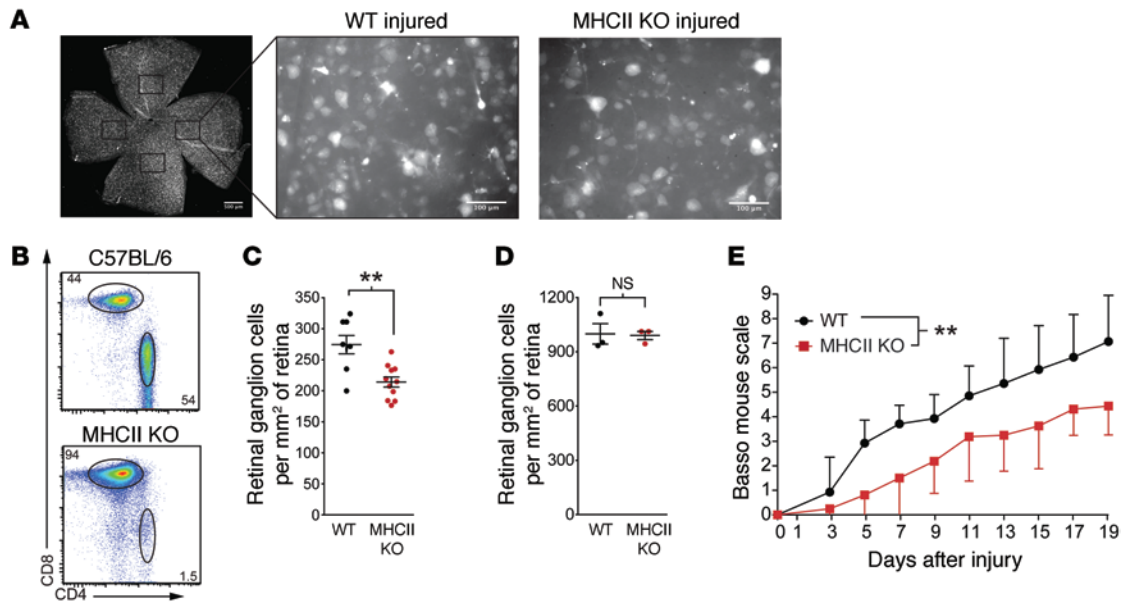
Figure 1. MHCII KO mice without CD4+ T cells display poor outcomes after CNS injury. (**A**) Representative images from wild-type or MHCII KO retinas labeled with the retrograde tracer Fluoro-Gold. Images are from retinas 7 days after injury. Scale bar: 500 μm (retina whole mount); 100 μm (individual field). (**B**) Representative flow cytometry plots of CD4+ and CD8+ lymphocytes in the deep cervical lymph nodes of C57BL/6 or MHCII KO mice. (**C**) RGC survival after optic nerve crush injury in MHCII KO or wild-type mice assessed 7 days after injury by Fluoro-Gold staining (n = 8, wild-type; n = 11, MHCII KO; representative of 2 experiments). (**D**) RGC counts (mean ± SEM) in the contralateral retinas of MHCII KO or wild-type mice (n = 3, wild-type; n = 3, MHCII KO, representative of 2 experiments). (**E**) Locomotor scores of C57BL/6 or MHCII KO mice after a 70-kDy impact below the T9-T10 vertebra was assessed by a blinded observer using the Basso mouse scale (n = 7, C57BL/6; n = 8, MHCII KO; representative of 2 experiments). (**C** and **D**) **P < 0.01, 2-tailed Student's t test. (**E**) **P < 0.01, repeated-measure 2-way ANOVA with Bonferroni's post-test. Error bars represent SEM.

potentiates neurotrophin signaling on injured neurons through neuronal IL-4 receptors and, thus, directly promotes neuronal survival and sprouting. These results alter the view of antigen specificity in the injury-induced T cell response and provide a role for injured tissue–derived molecular mediators in shaping the neuroprotective adaptive immune response.

Results

The accumulation of T cells in the injured CNS has been previously shown (15), although what leads to T cell activation and the requirement for MHCII-TCR interaction for their neuroprotective phenotype are not well understood. Since autoimmune T cells can be destructive, such as in autoimmune diseases, we hypothesized that there may be an alternative protective signaling pathway in CD4+ T cells that would lead to a neuroprotective response to injury. To distinguish between antigen-specific and "alternative" activation of T cells after CNS injury, we first used major histocompatibility class II (MHCII) knockout mice (*H2-Ab1−/−H2-Aa−/−H2-Eb1−/−H2-Eb2−/−H2-Ea−/−* mice; herein referred to as MHCII KO mice).

Since MHCII is required for CD4+ T cell development, activation, and long-term survival, these mice do not contain conventional CD4+ T cells but only a small population of CD4+ T cells with limited TCR diversity that recognize antigen in an antibody-like fashion (16); in contrast, their CD8+ T cell and B cell repertoires are normal (Supplemental Figure 1; supplemental material available online with this article; doi:10.1172/JCI76210DS1). Prior to readministration of T cells into MHCII KO mice, we examined their baseline spontaneous response to

CNS injury. We used a well-established and highly reproducible mouse model of acute optic nerve crush injury to quantitatively determine the effects on survival of the parent cell bodies of optic nerve axons, i.e., the retinal ganglion cells (RGCs) at 1 week after injury (Figure 1A). As expected from previous studies with different T cell–deficient animals (17), MHCII KO mice that are missing CD4+ T cells (Figure 1B) exhibited reduced neuronal survival compared with that of background-matched wild-type mice (Figure 1C; contralateral retinas with uninjured optic nerves did not differ in RGC counts, Figure 1D).

To determine whether the lack of CD4+ T cells also affects functional recovery from CNS injury, we used a calibrated spinal cord contusion injury at the T9-T10 vertebra and measured hind limb functional recovery with the Basso mouse scale (18). In line with the optic nerve injury experiments, MHCII KO mice displayed worse functional recovery compared with that of their wild-type counterparts (Figure 1E). These results suggest that endogenous conventional CD4+ T cells are indeed vital for immune-mediated neuroprotection and recovery after CNS injury.

To address our question of whether antigen recognition by T cells is essential to their neuroprotective response, we transferred CD4+ T cells from naive C57BL/6 mice into MHCII KO mice. This transferred CD4+ population is unable to be maintained in the periphery due to the lack of MHCII in these mice; however, in line with previous reports (19), the cells survived for a week in the recipient mice (Figure 2, A and B). Surprisingly, mice that received CD4+ T cells displayed significantly more surviving neurons after optic nerve crush injury than vehicle-treated MHCII KO mice lacking CD4+ T cells (Figure 2C; RGC counts in contralateral retinas
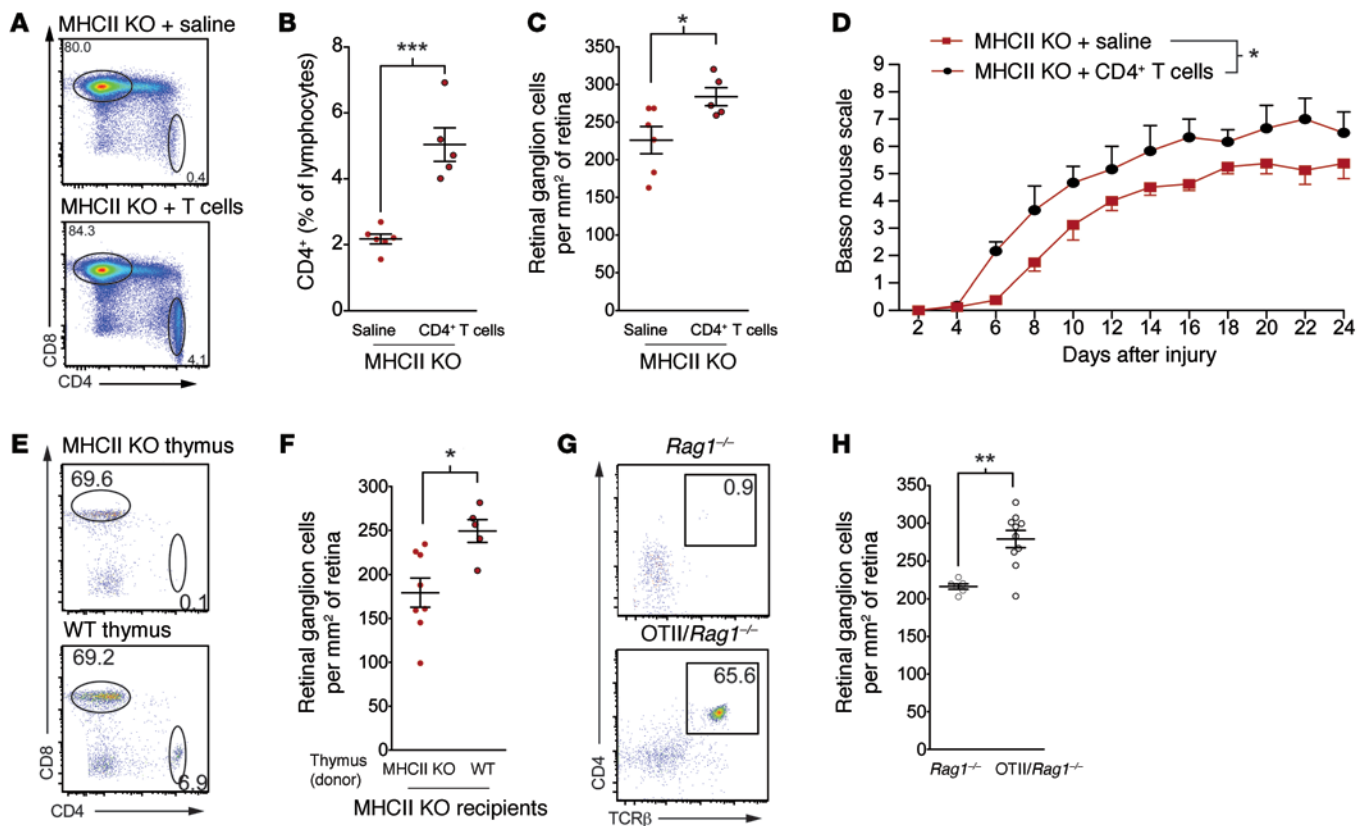
Figure 2. Antigen specificity is not required for CD4⁺ T cell–mediated neuroprotection. (**A**) Representative flow cytometry plots and (**B**) quantification of the deep cervical lymph nodes of control or CD4⁺ T cell–injected MHCII KO mice ($n = 5$, MHCII KO; $n = 6$, MHCII KO + CD4⁺ T cells; representative of 2 experiments). (**C**) RGC survival after optic nerve crush injury in MHCII KO mice injected with vehicle or CD4⁺ T cells on the day of injury ($n = 5$, MHCII KO; $n = 6$, MHCII KO + CD4⁺ T cells; representative of 2 experiments). (**D**) Locomotor score of MHCII KO mice injected with vehicle or CD4⁺ T cells ($n = 4$ mice per group; representative of 2 experiments). (**E**) Representative flow cytometry plots of CD4⁺ and CD8⁺ lymphocytes in the deep cervical lymph nodes of MHCII KO mice implanted with either MHCII KO or wild-type thymi. (**F**) RGC survival of MHCII KO mice implanted with either MHCII KO or wild-type thymi ($n = 5$, wild-type thymus; $n = 8$ MHCII KO thymus; representative of 2 experiments). (**G**) Representative flow cytometry plots of CD4⁺ lymphocytes in the deep cervical lymph nodes of $Rag1^{-/-}$ or OTII/$Rag1^{-/-}$ mice. (**H**) RGC survival of $Rag1^{-/-}$ and OTII/$Rag1^{-/-}$ mice assessed 7 days after injury ($n = 6$, $Rag1^{-/-}$; $n = 10$, OTII/$Rag1^{-/-}$; representative of 3 experiments). (**B**, **C**, **F**, and **H**) *$P < 0.05$, **$P < 0.01$, ***$P < 0.001$, 2-tailed Student's t test. (**D**) *$P < 0.05$, repeated-measure 2-way ANOVA. Error bars represent SEM.

did not differ between the groups, Supplemental Figure 2A). To determine whether antigen specificity is also dispensable for CD4⁺ T cell–mediated functional recovery from spinal cord injury, we transferred MHCII KO mice with CD4⁺ T cells from naive C57BL/6 mice or vehicle at both 1 day after spinal cord contusive injury and 8 days after spinal cord injury. As with optic nerve injury, mice that received CD4⁺ T cells exhibited greater functional recovery from spinal cord injury than mice that were treated with saline (Figure 2D).

To confirm that the phenotype that we observed was not due to activation of CD4⁺ T cells in their naive host or due to adoptive transfer, we repeated the study using a model in which CD4⁺ T cells were allowed to develop in vivo in MHCII KO mice. To this end, we transplanted P2 thymi from wild-type or MHCII KO donors under the kidney capsules of 3-week-old MHCII KO recipients. These exogenous thymi were implanted 6 weeks before optic nerve injury to allow enough time for sufficient production of CD4⁺ T cells. In agreement with the previously published works (20), introduction of the wild-type thymi allowed the MHCII KO recipients to generate endogenous CD4⁺ T cells (Figure 2E). Although wild-type thymi-transplanted mice now had mature T cells, these cells were

unable to interact with endogenous antigen-presenting cells due to the MHCII deficiency in the host and, thus, they were not able to respond to antigenic stimuli. MHCII KO recipients of MHCII KO thymi were unable to generate mature T cells and served as negative control. Once the mice had developed CD4⁺ T cells, they underwent optic nerve injury. Mice that received wild-type thymi, and thus developed CD4⁺ T cells, displayed significantly more surviving neurons than the recipients of MHCII KO thymi that did not possess CD4⁺ T cells (Figure 2F; RGC counts in contralateral retinas did not differ between the groups, Supplemental Figure 2B). These results further suggest that mature CD4⁺ T cells can exert a beneficial effect after sterile injury, even in the absence of recognition of their cognate antigen.

As an alternate method of studying the role of antigen-nonspecific T cells in CNS injury, we also examined neuronal survival in TCR transgenic mice bearing only ovalbumin-specific CD4⁺ T cells on a $Rag1^{-/-}$ background (OT-II/$Rag1^{-/-}$ mice). These OT-II/$Rag1^{-/-}$ mice, which lack the entire adaptive immune system except for a population of CD4⁺ T cells specific for ovalbumin (Figure 2G), exhibited an enhanced neuroprotective response after
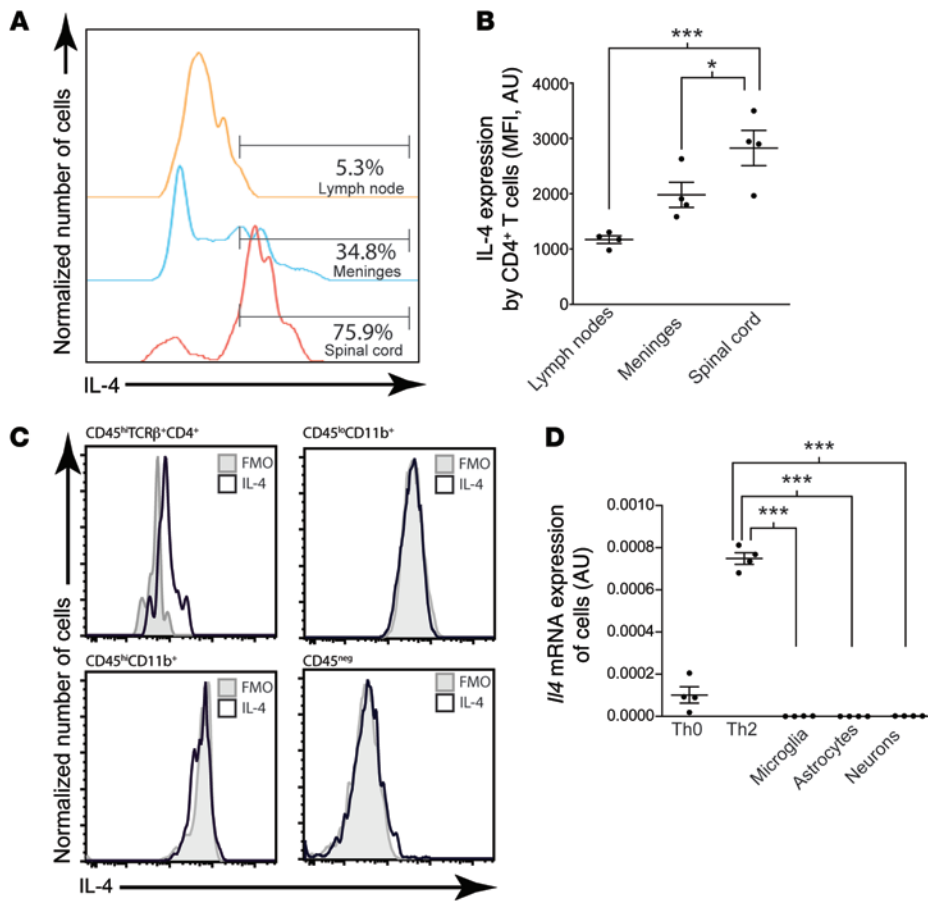
Figure 3. CD4+ T cells produce IL-4 in the CNS after injury. (**A**) Representative histograms and (**B**) quantification of IL-4–expressing CD4+ T cells from the lymph nodes, meninges, and spinal cords of C57BL/6 mice after contusion injury ($n = 4$ per group; representative of 3 experiments). (**C**) Representative histograms showing IL-4 expression in CD4+ T cells, CD45^{hi}CD11b+ macrophages, CD45^{lo}CD11b+ microglia, or CD45$^-$ resident CNS cells in the spinal cords of C57BL/6 mice after contusion injury. Gray histograms indicate flow minus one (FMO) controls. (**D**) *Il4* mRNA expression of cultured cells, normalized to expression of *Gapdh* ($n = 4$ per group; representative of 2 experiments). *$P < 0.05$, ***$P < 0.001$, 1-way ANOVA with Bonferroni's post-test. Error bars represent SEM.

optic nerve crush compared with that of *Rag1$^{-/-}$* background controls (Figure 2H; RGC counts in contralateral retinas did not differ between the groups, Supplemental Figure 2C), further indicating that cognate antigen recognition is not prerequisite for T cells to acquire their neuroprotective properties after CNS injury.

In search for a better understanding of molecular mechanism underlying T cell–mediated neuroprotection and recovery, we analyzed the cytokines that T cells from the injured spinal cord produced and found that one of the major cytokines produced by T cells at the site of injury was IL-4. Interestingly, we found more IL-4–producing T cells at the site of injury than in the lymph nodes or even in the meninges (Figure 3, A and B), a compartment that is known for its IL-4–skewed environment (21, 22). T cells from the injury site were the major source for IL-4 production, as compared with any other cells in the injured CNS (Figure 3C). To further confirm that IL-4 production in the spinal cord is due to CD4+ T cells, we examined cultured CD4+ T cells, microglia, astrocytes, and neurons for IL-4 expression. While Th0 cells in vitro expressed abundant *Il4* mRNA and this expression was further increased by culturing the cells in Th2-skewing conditions, there was a lack of *Il4* expression by resident nonimmune CNS cells, i.e., astrocytes, neurons, and oligodendrocytes (Figure 3D). Although these cells were tested in the culture conditions and could potentially upregulate IL-4 after injury, the results in Figure 3C suggest that injury does not induce IL-4 in neural cells.

Due to shared signaling pathways used by both IL-4 and growth factors, such as neurotrophins and IGF1 (through IRS1/2 signaling; refs. 23, 24), and since IL-4 has been implicated pre-viously in the healthy (21) and injured (25) CNS, it was reasonable to assume that it could be acting as a T cell–derived neuroprotective molecule. To address the role of IL-4 on neuronal survival after CNS injury, we used again the optic nerve crush injury model to compare neuronal survival between *Il4$^{-/-}$* mice and background-matched wild-type controls. *Il4$^{-/-}$* mice exhibited impaired neuronal survival as compared with that of their wild-type counterparts (Figure 4A; RGC counts in contralateral retinas did not differ between the groups, Supplemental Figure 2D). Importantly, CD4+ T cell infiltration into the injured tissue was not affected in *Il4$^{-/-}$* mice (Figure 4B). To test whether the protective IL-4 is indeed produced by the immune cells, we transplanted *Il4$^{-/-}$* or wild-type bone marrow into irradiation-conditioned wild-type hosts. After the bone marrow had fully engrafted (peripheral engraftment at >90%), mice underwent optic nerve injury. Recipients of *Il4$^{-/-}$* bone marrow demonstrated impaired neuronal survival as compared with that of control mice that received wild-type bone marrow (Figure 4C; RGC counts in contralateral retinas did not differ between the groups, Supplemental Figure 2E). To further ensure that the neuroprotective IL-4 originated from CD4+ T cells, we injected acutely isolated IL-4–deficient CD4+ T cells (from *Il4$^{-/-}$* donors) or IL-4–sufficient CD4+ T cells (from wild-type donors on the same genetic background) into *Rag1$^{-/-}$* (T cell–deficient) mice and subjected these mice to optic nerve crush injury 3 weeks later. Wild-type CD4+ T cells led to a higher neuronal survival in *Rag1$^{-/-}$* hosts than *Il4$^{-/-}$* T cells (Figure 4D; RGC counts in con-
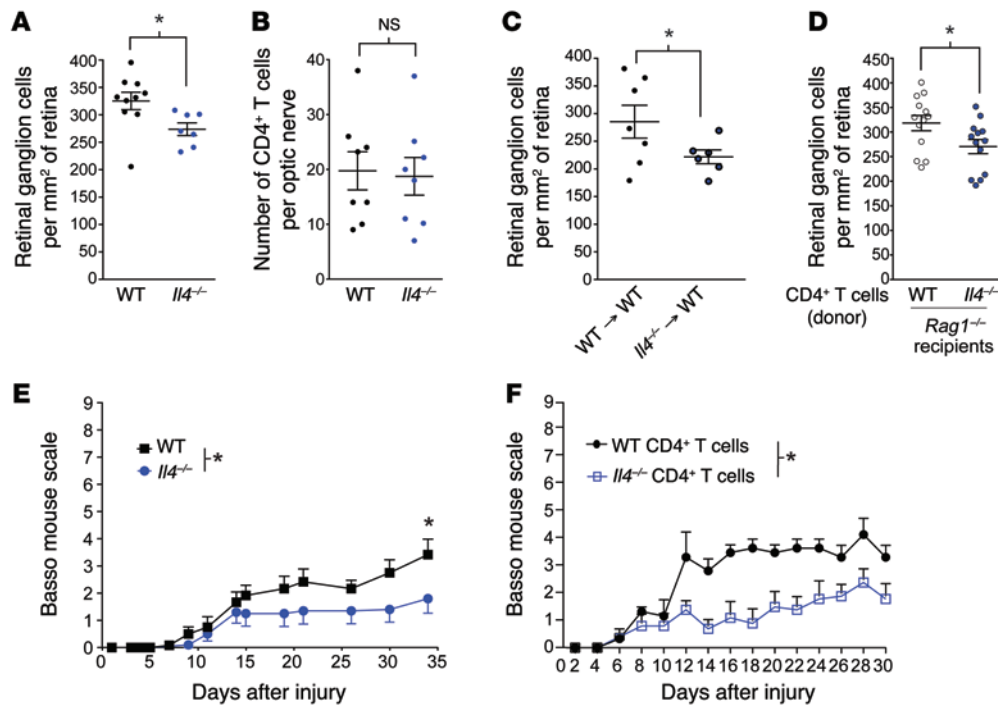
Figure 4. IL-4–producing CD4+ T cells mediate neuroprotection after CNS injury. (**A**) Scatter plots represent RGC survival of $Il4^{-/-}$ or wild-type mice ($n = 10$, wild-type; $n = 7$, $Il4^{-/-}$; representative of 2 experiments). (**B**) Scatter plots represent the number of CD4+ T cells that infiltrated into the CNS parenchyma of $Il4^{-/-}$ or wild-type mice ($n = 8$ per group; representative of 2 experiments). (**C**) RGC survival of wild-type → wild-type or $Il4^{-/-}$ → wild-type bone marrow chimeras assessed 7 days after injury ($n = 7$, wild-type bone marrow; $n = 6$, $Il4^{-/-}$ bone marrow; representative of 2 experiments). (**D**) RGC survival of $Rag1^{-/-}$ mice injected with either wild-type or $Il4^{-/-}$ CD4+ T cells. RGC survival was quantified 7 days after injury ($n = 13$ wild-type and $Il4^{-/-}$ T cell injected; representative of 2 experiments). (**E**) Locomotor score of wild-type and $Il4^{-/-}$ mice that have undergone a spinal cord injury ($n = 6$, wild-type; $n = 10$, $Il4^{-/-}$; representative of 2 experiments). (**F**) Locomotor score of $Rag1^{-/-}$ mice reconstituted with either wild-type or $Il4^{-/-}$ CD4+ T cells from naive mice that have undergone a spinal cord injury ($n = 4$ per group; representative of 2 experiments). (**A–D**) *$P < 0.05$, 2-tailed Student's t test. (**E** and **F**) *$P < 0.05$, repeated-measure 2-way ANOVA with Bonferroni's post-test. Error bars represent SEM.

tralateral retinas did not differ between the groups, Supplemental Figure 2F), suggesting that the primary source of neuroprotective IL-4 after injury is indeed the CD4+ T cells.

To determine whether the neuroprotective effect of IL-4 would also affect functional recovery, we performed spinal cord injury on $Il4^{-/-}$ mice and wild-type controls. As expected from the optic nerve injury model, $Il4^{-/-}$ mice displayed a deficit in functional recovery from spinal cord injury (Figure 4E). Additionally, we transferred wild-type or $Il4^{-/-}$ CD4+ T cells into $Rag1^{-/-}$ mice. The T cells were allowed to engraft in the recipients for 3 weeks before we performed spinal cord injury. $Rag1^{-/-}$ mice that received wild-type T cells exhibited enhanced functional recovery from spinal cord injury compared with those mice that received $Il4^{-/-}$ CD4+ T cells, confirming that a neuroprotective CD4+ T cell response is IL-4 mediated (Figure 4F).

Two mechanistic questions remained unanswered: what induces T cells at the site of injury to express IL-4 and how does IL-4 mediate neuroprotection and recovery?

To address the mechanism underlying the Th2 skew at the site of injury, we established an in vitro system in which CD4+ lymphocytes from cervical lymph nodes were incubated with isolated optic nerves (in the presence of the CD4− fraction from the lymph node serving as antigen-presenting cells). Because our findings indicated that the induction of a neuroprotective T cell response does not require MHCII-TCR interactions (Figure 1),

we postulated that soluble factors from the injured CNS induce a Th2 phenotype directly on T cells. To assess Th2 skewing in wild-type T cells, we measured a master transcriptional regulator of Th2 cells, $Gata3$ (26), by real-time quantitative PCR. Isolated CD4+ lymphocytes were incubated with CD4− antigen-presenting cells and injured optic nerves for 3 days, after which an increase in $Gata3$ in CD4+ T cells was evident (Figure 5A), suggesting a Th2 skew by factors within the CNS tissue. Although $Gata3$ is a master regulator of Th2 skew, we also assessed more direct measurements of IL-4 in these cells. Since IL-4 is a difficult cytokine to measure and due to its 2-step production process (27), protein levels of IL-4 are the only reliable measure. To this end, we first used T cells from reporter KN2 mice. KN2 is a reporter mouse line, which expresses human CD2, indicating IL-4 protein translation (27). Incubation of KN2-derived T cells with injured CNS tissue indeed showed an increase in T cell–derived IL-4 production (Figure 5, B and C). Additionally, flow cytometric analysis of intracellular staining for IL-4 in cultured T cells (directly assessing IL-4 production) also demonstrated an increase in IL-4 production upon incubation with optic nerves (Figure 5, D and E), suggesting that the optic nerve tissue is sufficient to drive a Th2 response in CD4+ T cells.

Since we detected a correlation between IL-4 expression by T cells and their $Gata3$ expression and due to a robustness of $Gata3$ assessment by qPCR, we proceeded with our studies to
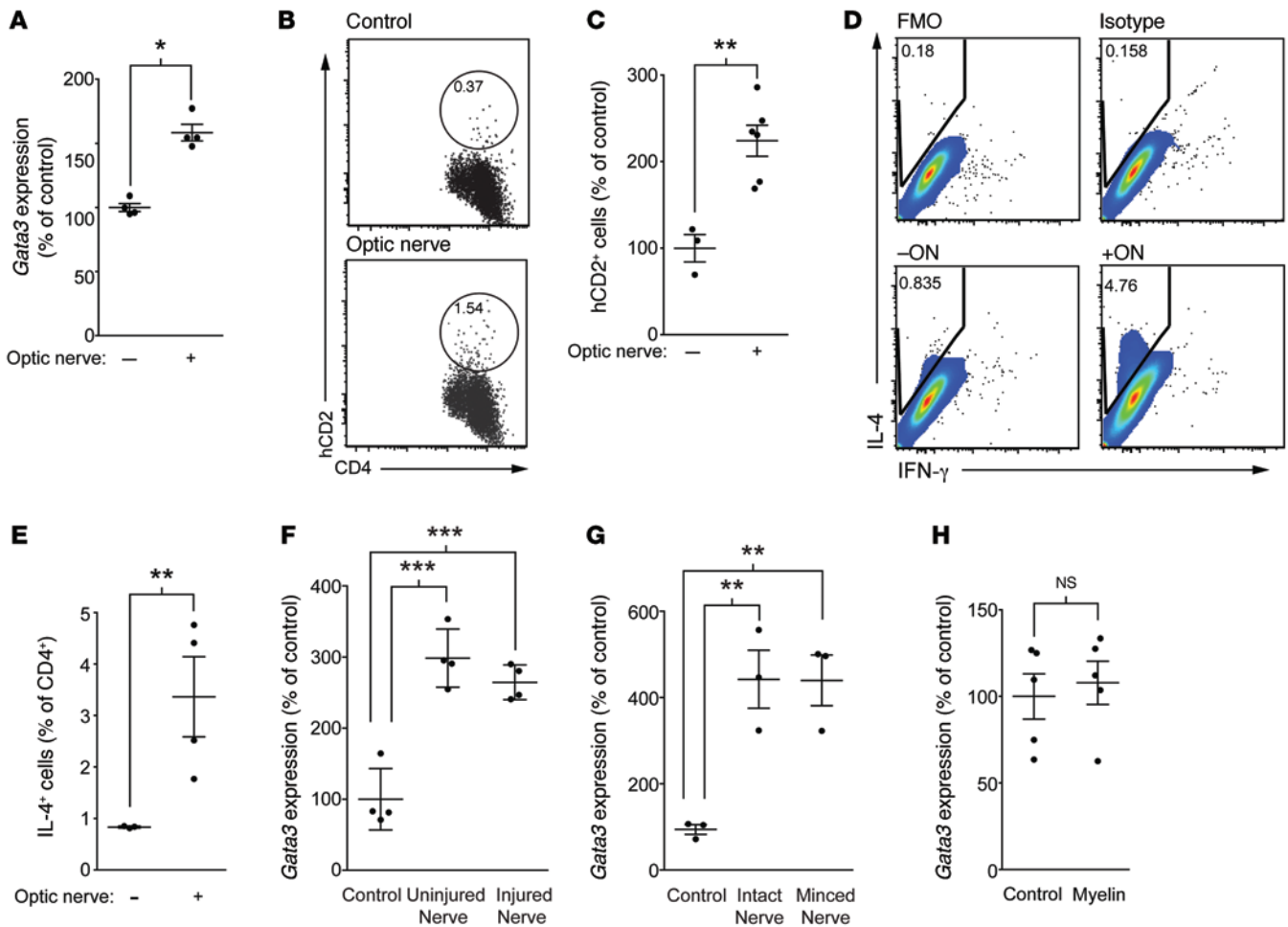
Figure 5. CNS tissue skews T cells toward a Th2 phenotype. (**A**) CD4+ T cells from total lymph nodes were incubated with optic nerves and antigen-presenting cells. After culture, CD4+ T cells were resorted and *Gata3* expression analyzed using qRT-PCR (relative to *Gapdh*) (n = 3 per group; representative of >3 experiments). (**B**) Representative flow cytometry plots and (**C**) quantification of human CD2 (hCD2) expression (reporter for IL-4 protein; KN2 mice) in cultures of lymph node cells incubated with or without optic nerves (n = 3, control; n = 7, optic nerve; representative of 2 experiments). (**D**) Representative flow cytometry plots and (**E**) quantification of IL-4+CD4+ T cells in cultures of lymph node cells incubated with or without optic nerves, as a percentage of CD4+ T cells (n = 4, control; n = 4, optic nerve; representative of 3 experiments). (**F**) *Gata3* expression in sorted CD4+ T cells after culture in the presence of optic nerves isolated from either injured or naive mice (n = 4 per group; representative of 2 experiments). (**G**) *Gata3* expression in the presence of optic nerves that had been minced or left intact (n = 3 per group; representative of 2 experiments). (**H**) CD4+ T cells from deep cervical lymph nodes and antigen-presenting cells were incubated in the presence or absence of 80 μg of myelin vesicles before CD4+ T cells were resorted and assayed for *Gata3* relative to *Gapdh* (n = 5 per condition; representative of 2 experiments). (**A**, **C**, **E**, and **H**) *P < 0.05, **P < 0.01, 2-tailed Student's *t* test. (**F** and **G**) **P < 0.01, ***P < 0.001, 1-way ANOVA with Bonferroni's post-test. Error bars represent SEM.

identify the "factor" that leads to IL-4 production using *Gata3* as an expression readout. Of note, optic nerves isolated from 3-day optic nerve–injured or naive mice resulted in similar degrees of *Gata3* induction in T cells (Figure 5F), suggesting that the factor(s) is produced acutely after injury caused by excision of the optic nerves. To determine whether additional "damage" to the nerve is necessary to promote this phenotype or whether removal from the mouse causes sufficient damage to drive the Th2 response, we cultured nerves that had been minced or left intact and found that the damage to the axons from removal of the nerves from their hosts was sufficient to drive the *Gata3* induction in CD4+ T cells (Figure 5G).

As we did not see a requirement for antigen specificity of CD4+ T cells in order for them to become protective in vivo, we asked whether antigen specificity played a role in this Th2 skew in vitro.

Therefore, we first cultured T cells with myelin, which contains many of the antigens that have been implicated in T cell autoimmunity to the CNS. However, purified myelin did not have any effect on *Gata3* expression in CD4+ T cells (Figure 5H).

Since in vivo MHCII recognition was not needed for the T cell–mediated beneficial response, we replaced the wild-type antigen-presenting cells (CD4− fraction) with MHCII KO antigen-presenting cells in our cultures of wild-type T cells to determine whether MHCII signaling on antigen-presenting cells was necessary for the induction of Th2 skewing by CNS tissue. Indeed, MHCII deficiency on antigen-presenting cells did not affect *Gata3* induction in CD4+ T cells in response to incubation with the injured optic nerve (Figure 6A). Similarly, T cells derived from OTII/*Rag1*−/− mice and, therefore, not responding to any of the antigens present in the injured tissue also demonstrated upregulation of *Gata3*
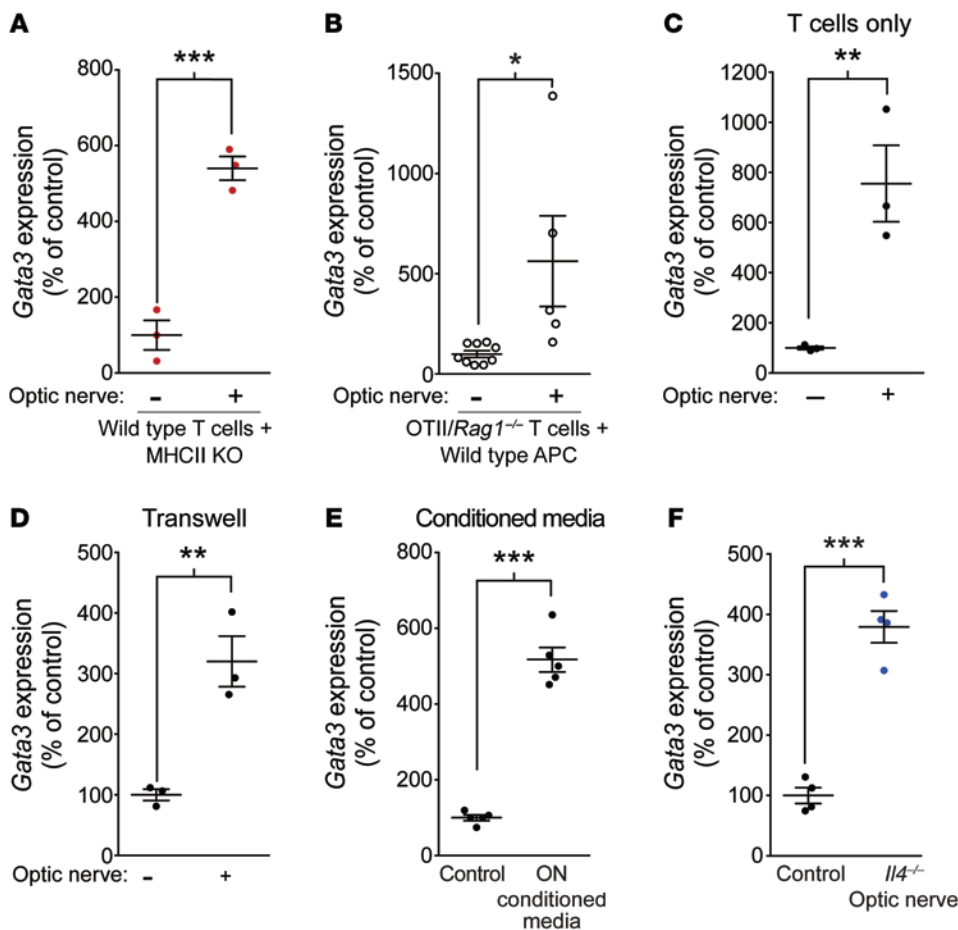
Figure 6. CNS tissue does not mediate the effects on CD4+ T cells through antigen or IL-4. (**A**) *Gata3* expression in sorted wild-type CD4+ T cells cocultured with MHCII KO antigen-presenting cells in the presence or absence of optic nerves from uninjured mice (*n* = 3 per group; representative of 2 experiments). (**B**) *Gata3* expression in sorted OTII/*Rag1*−/− CD4+ T cells cocultured with wild-type antigen-presenting cells in the presence or absence of optic nerves from uninjured mice (*n* = 9 wild-type; *n* = 5 OTII/*Rag1*−/−; representative of 2 experiments). (**C**) *Gata3* expression in sorted wild-type CD4+ T cell cultures lacking antigen-presenting cells incubated in the presence or absence of optic nerves from uninjured mice (*n* = 3 per group; representative of >3 experiments). (**D**) *Gata3* expression in sorted CD4+ T cells after culture in the presence or absence of isolated optic nerves placed in a Transwell with 0.4-μm pores (*n* = 3 per group; representative of 2 experiments). (**E**) *Gata3* expression in sorted CD4+ T cells after culture in optic nerve–conditioned media or control media (*n* = 5 per group; representative of 2 experiments). (**F**) *Gata3* expression (mean ± SEM) in sorted CD4+ T cells after culture in the presence or absence of isolated optic nerves from *Il4*−/− mice (*n* = 4 per group; representative of 2 experiments). *P < 0.05; **P < 0.01; ***P < 0.001, 2-tailed Student's *t* test used for statistical analysis. Error bars represent SEM.

after incubation with the injured optic nerves (Figure 6B). Moreover, removal of antigen-presenting cells from the cultures of T cells with the optic nerves did not affect the induction of *Gata3* in T cells (Figure 6C), suggesting that the factor originating from the injured CNS interacts directly with T cells and skews them to the Th2 lineage. To determine whether there was a cellular interaction that was causing this upregulation of *Gata3* or whether there was a soluble factor that was mediating the effects of optic nerves on T cells, we cultured CD4+ T cells with optic nerves that were separated from the T cells by 0.4-μm Transwell. Optic nerves were able to upregulate *Gata3* mRNA in CD4+ T cells, even through Transwell separation (Figure 6D), suggesting that soluble factors originating in the injured CNS were responsible for this effect. To confirm this phenotype, we conditioned media with optic nerve explants for 3 days. The media was then added to T cell cultures after being passed through a 0.22-μm filter. As expected, conditioned media was also able to induce the upregulation of *Gata3* in T cells (Figure 6E). To rule out the possibility that the optic nerves could be producing IL-4 themselves to mediate this effect, we used optic nerves from *Il4*−/− mice, and a similar degree of *Gata3* induction was achieved (Figure 6F).

We hypothesized that the Th2 skewing is induced via molecular patterns/mediators or "alarmins" (28) originating from the damaged tissue. Pattern recognition is mediated by unique receptors, such as TLRs, among other pattern recognition receptors (29). Many

TLRs signal through a common signaling molecule, MyD88, which mediates downstream transcriptional activation by several mechanisms (30). To address a possible role of MyD88 signaling in CNS-induced Th2 skewing, we used T cells from wild-type or *Myd88*−/− mice incubated with the optic nerves. Whereas T cells from wild-type mice demonstrated, as expected, upregulation of *Gata3*, no such upregulation was detected in the cultures with *Myd88*−/− T cells (Figure 7A), suggesting that the signaling pathway that results in Th2 skewing is mediated, at least in part, via MyD88 intrinsic to T cells.

To determine whether the myriad of molecular "alarmins" that are released and signal from the injured CNS induce a desired neuroprotective T cell response in vivo, we isolated T cells from the injured spinal cords of wild-type and *Myd88*−/− mice and looked at intracellular cytokine expression. While there was high expression of IL-4 in wild-type T cells, *Myd88*−/− mice exhibited lower amounts of IL-4 (Figure 7, B and C). Of note, IL-4 expression was not completely eliminated in *Myd88*−/− mice, suggesting that other MyD88-independent pathways may play a role in the induction of IL-4 expression after spinal cord injury. To examine whether MyD88 signaling is physiologically relevant to a neuroprotective immune response after injury, we examined optic nerve injury in *Myd88*−/− mice and found that their neuronal survival was indeed significantly impaired compared with that of control mice (on identical genetic background with sufficient MyD88 expression) (Figure 7D; RGC counts in contralateral retinas did not differ between the
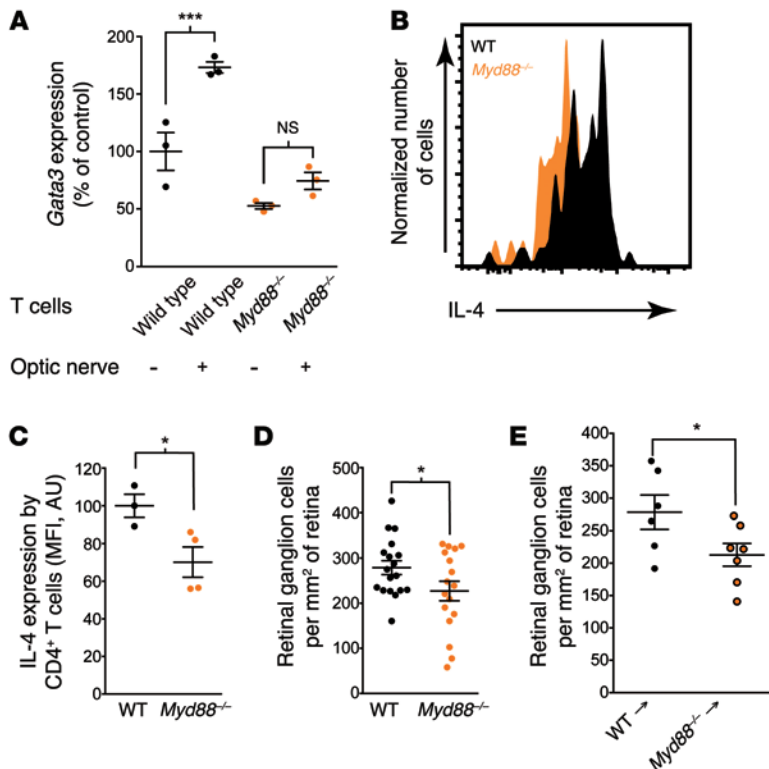
Figure 7. MyD88-dependent Th2 skewing. (**A**) *Gata3* expression in sorted wild-type or *Myd88*−/− CD4+ T cells cultured with optic nerves from uninjured mice (n = 3 per group; representative of 2 experiments). (**B**) Representative histograms and (**C**) quantitation of IL-4 expression in CD4+ T cells from the spinal cords of C57BL/6 and *Myd88*−/− mice after contusion injury (representative of 2 experiments). (**D**) RGC survival of wild-type and *Myd88*−/− mice 7 days after optic nerve injury (n = 18, wild-type; n = 17, *Myd88*−/−; representative of 2 experiments). (**E**) RGC survival of wild-type → wild-type or *Myd88*−/− → wild-type bone marrow chimeras 7 days after injury (n = 6, wild-type bone marrow recipients; n = 7, *Myd88*−/− bone marrow recipients; representative of 2 experiments). (**A**) ***P < 0.001, 1-way ANOVA with Bonferroni's post-test. (**C**–**E**) *P < 0.05, 2-tailed Student's t test. Error bars represent SEM.

groups, Supplemental Figure 2G). Bone marrow transplantation from *Myd88*−/− or wild-type donors into irradiation-conditioned wild-type recipients recapitulated the results obtained with germline knockout mice (Figure 7E; RGC counts in contralateral retinas did not differ between the groups, Supplemental Figure 2H), further pointing to the importance of the immune cells as responders to MyD88-dependent signals.

To determine what factor(s) might be playing a role in inducing Th2 skewing after CNS injury, we tested a panel of MyD88-dependant TLR ligands. Much to our surprise, none of the tested TLR ligands increased *Gata3* in T cells, and several decreased its expression instead (Supplemental Figure 3). The IL-1 family of cytokines (IL-1α, IL-1β, IL-18, and IL-33) all signal in an MyD88-dependent manner (31) and may mediate the effect either collectively or synergistically. Future studies should focus on addressing the role of these cytokines as well as looking for additional players in the injured CNS that may lead to induction of neuroprotective IL-4–producing T cells.

Importantly, to address the molecular mechanism of IL-4–mediated beneficial affect on injured neurons, we used a well-established and robust ex vivo axonal outgrowth model using cortical explant cultures (ECs), allowing for the analysis of soluble factors on outgrowth in an organotypic setting (ref. 32 and Figure 8A). This model, while not an in vivo system, better mimics the in vivo condition than isolated neuronal cultures, which lack the glial compartment that plays an important role in proper axonal outgrowth. Furthermore, the physiological connections of the entorhinal cortex, which have already been established in vivo by the time of tissue excision (postnatal day 2–3), need to be severed in order to produce the ECs, and thus the outgrowth is a response of the damaged neurons attempting to reconnect to their physiologic target. IL-4–producing Th2 cells obtained by an antigen-

independent stimulation protocol (concanavalin [ConA] activation) and kept in a collagen matrix next to the slice increased axonal outgrowth in this ex vivo model, whereas Th1 cells failed to do so (Figure 8B). In order to define the impact of IL-4 on axons, induction of outgrowth by Th2 cells served as a readout assay for our further analyses. In fact, axonal outgrowth achieved by Th2 cells was inhibited by the addition of an IL-4–neutralizing antibody (Figure 8C) but remained unaffected by neutralization of either IL-10 or IL-13 (Figure 8D), strongly suggesting that IL-4 is a key Th2-derived molecule that mediates the effect. To ensure that this response was specific to IL-4 signaling on the EC slices, we examined Th2 cells cocultured with EC slices from *Il4r*−/− mice. In contrast to control EC slices, Th2-skewed cells were not able to induce axonal outgrowth in slices from *Il4r*−/− mice (Figure 8E).

To further demonstrate that IL-4–induced outgrowth after lesion in the ex vivo model results in sprouting into the proper target tissue, we cultured EC slices from β-actin-*EGFP* mice with wild-type hippocampal slices (33) to determine whether application of recombinant IL-4 would increase the regrowth of axons from the EC through their physiological route, the perforant path, into the hippocampus (Figure 8F). Indeed, exogenous IL-4 was able to potentiate axonal ingrowth (EGFP+ axons) into the hippocampus (Figure 8G).

To determine whether IL-4 could be signaling directly to neurons, we first examined whether neurons express the correct receptor for binding IL-4. In cultured neurons, IL-4Rα can be found as mRNA and protein (Figure 8, H and I). We next examined whether IL-4 could directly signal to neurons to promote axon elongation using cultures of cortical neurons that were treated with IL-4. Indeed, treatment of neuronal cultures with IL-4 promoted enhanced elongation of axons when compared with cultures treated with vehicle (Supplemental Figure 4), suggesting that IL-4 signaling directly to neurons could be promoting this Th2-driven axonal outgrowth seen in our slice cultures. To test this hypothesis, we cultured Th2 cells with wild-type or *Camk2g-Cre Il4r*fl/fl slices (in which only neurons are deficient in IL-4R, while other neural cells in the slices are expressing their regular levels of IL-4R). Whereas slices from wild-type mice showed, as expected, axonal outgrowth in response to Th2 (but not Th1) cells, slices from *Camk2g-Cre Il4r*fl/fl mice showed no such response to Th2 cells (Figure 8J), indicating that IL-4 signals directly through neuronal IL-4R.

As mentioned above, IL-4 can act via a signaling pathway shared with growth factors, including neurotrophins, through the IRS family of adaptor proteins (23, 24), which influences signal transduction through AKT and MAPK signaling. Interestingly, a previous study showed no indications for a relevant role of endogenous neurotrophins in the initiation of axon outgrowth from cortical explants. However, application of recombinant NT-3 potentiated this spontaneous outgrowth (33), pointing to a role of neurotrophins in strengthening the signaling in the preactivated axonal growth pathway. To determine whether this potentiation of neurotrophin signaling is involved in IL-4–mediated axonal outgrowth, we tested axonal outgrowth induced by Th2 cells after blocking the neurotrophin signaling. Indeed, we found that inhibitory antibodies to neurotrophins involved in outgrowth from EC cultures (34) were effective in abolishing Th2-mediated axonal outgrowth (Figure 9A).

To determine whether there is crosstalk between IL-4 and neurotrophin signaling at the level of the AKT and MAPK pathways in neurons, we tested whether IL-4 pretreatment would potentiate this pathway in neurotrophin-treated neurons. Indeed, pretreatment with IL-4 elicited an increase in MAPK signaling in neurotrophin-treated cultures, as evidenced by an increase in phosphorylated MAPK44 to total MAPK44 (Figure 9, B and C). This effect was not present when $Il4r^{-/-}$ neurons were treated with IL-4 before neurotrophins were applied (Figure 9, B and D). Furthermore, blocking the AKT and MAPK signaling pathways downstream of IL-4R (35) and neurotrophin signaling (36) also abolished the Th2-induced outgrowth of axons in EC slice cultures (Figure 9E).

To determine whether IL-4 could be a relevant treatment for CNS injury, we examined whether the IL-4R is expressed in the relevant compartment of CNS neurons in vivo. As demonstrated in cultured neurons, expression of IL-4Rα was detectable on spinal axons, including those of the corticospinal tract (Figure 9F and Supplemental Figure 5).

To determine whether the IL-4–induced axonal outgrowth and IL-4R expression in the corticospinal tract could be harnessed therapeutically, we injected Th2 cells directly into the site of a mild spinal cord injury, with PBS- and Th1-injected mice serving as controls, and assayed the mice for axonal outgrowth and functional recovery. The locally injected T cells survived in the spinal cord and could be seen even 5 mm caudal of the injection site (Supplemental Figure 6). Despite the fact that wild-type mice already display a highly Th2-skewed environment in the injured spinal cord (Figure 3A), addition of exogenous Th2-skewed cells, but not Th1-skewed cells, was able to further potentiate axonal outgrowth of corticospinal tract axons 5 mm distal to the injury site (Figure 9, G and H) and to promote a significant increase in functional recovery from spinal cord injury (Figure 9I).

Discussion

Our results demonstrate that neuroprotection (studied after optic nerve crush injury), axon regrowth, and functional recovery (studied after spinal cord contusive injury), all benefit from an antigen-independent response of IL-4–producing T cells induced by local damage-associated molecules. Injured tissue, thus, induces a neuroprotective T cell response, which is MHCII independent and MyD88 dependent. IL-4–producing T cells promote recovery after CNS injury directly via neuronal IL-4 receptors, potentiating neurotrophin signaling to promote neuronal survival and regrowth (Figure 10).

Due to the potency of autoimmune T cells to promote neuroprotection (10), it has been assumed that the T cells that mediate neuroprotection after CNS injury need to be specific to CNS antigens. However, we show here that T cell–dependent neuroprotection does not necessarily require antigen recognition and neuroprotective T cell phenotype could be induced independently of MHCII. Although T cell specificity may be required for T cell migration to the injured tissue (37), our results demonstrate that, once at the site of injury, a neuroprotective Th2 skew can occur independent of antigen recognition.

Furthermore, our results do not exclude the possibility that CNS self-antigen–specific T cells exert a more potent neuroprotection than that of antigen nonspecific cells or that the endogenous CD4+ T cells that mediate neuroprotection in wild-type mice can be boosted by vaccination with CNS self antigen, as has been previously reported (13). Boost of CNS-reactive T cells may allow a higher amount of infiltration into the injured CNS, which can then be skewed by the injured tissue into a neuroprotective IL-4–producing phenotype and hence a higher degree of neuroprotection and recovery (38).

The results presented here suggest a mechanistic explanation to the phenomenon of T cell–mediated neuroprotection and recovery after CNS trauma. A better understanding of the actions of T cells after injury may have far-reaching clinical implications for the design of new treatment modalities for axonal damage in the course of CNS injuries, a progressive form of multiple sclerosis, and other neurodegenerative disorders by targeting the protective antigen-independent IL-4–producing T cells, while preventing destructive autoimmunity that commonly occurs with a CNS antigen-specific T cell response.

The T cell response to damage-associated molecules originating from the injured CNS is MyD88 dependent, although $Myd88$ knockout mice still show IL-4 production by T cells (albeit to a lesser extent). This suggests that additional pathways may be involved through which T cells respond to damage signals following injury. None of the tested TLR agonists were able to induce $Gata3$ expression in T cells. Since it is reasonable to hypothesize that several molecules originating from the injured CNS may influence T cells to induce a compensatory response in the CNS, future studies should concentrate on molecules such as the members of IL-1 cytokine family (IL-1α, IL-1β, IL-18, and IL-33), which exert their effects through MyD88 independently of TLRs. Importantly, the fact that neuroprotective T cells are induced in an MHCII-independent manner contrasts with a previous hypothesis that neuroprotective T cells need to be specific to brain antigens, i.e., autoimmune (10), and suggests that safe therapies targeting T cells may be developed in the future that avoid the risk of autoimmune disease development.

What makes the search for neuroprotective therapies after CNS injury especially pressing is that there currently are no neuroprotective treatments that have undergone rigorous testing in the clinical setting. While several small phase I trials held promise for treatments, such as hyperbaric oxygen treatment, progesterone treatment, and hypothermia, these treatments either have not yet
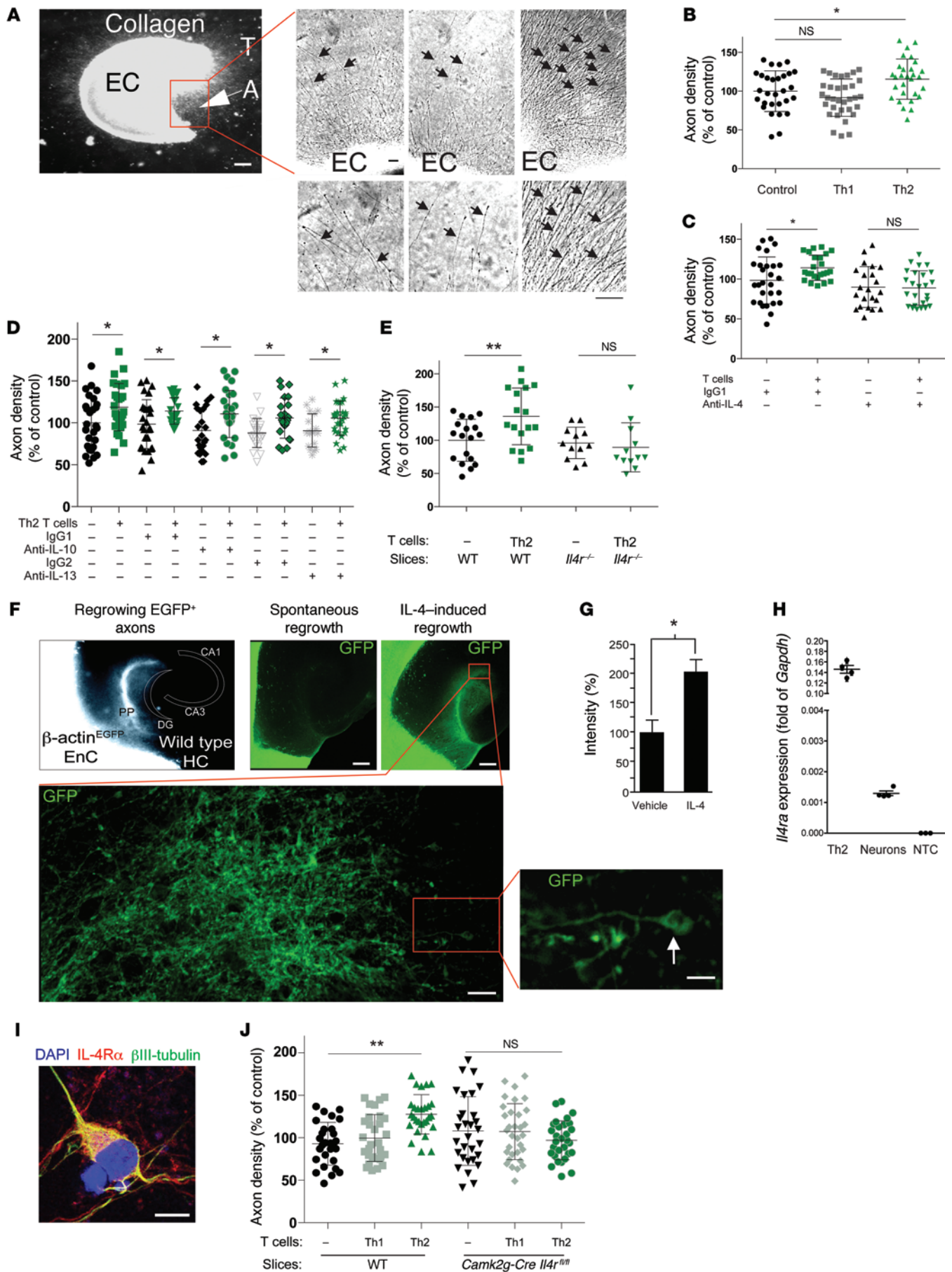
Figure 8. T cell–derived IL-4 acts on neurons to induce axonal regrowth.
(**A**) Cortical ECs with outgrowing axons (A) oriented toward the T cells (T). Scale bar: 300 μm. (**B**) Culture of Th2 cells with cortical ECs (*n* = 29–33 per condition). (**C**) Coculture of wild-type slices with activated Th2 cells in the presence of neutralizing anti–IL-4 antibody (*n* = 22–25 per condition). (**D**) Coculture of wild-type slices with activated Th2 cells in the presence of neutralizing anti–IL-10 or anti–IL-13 antibodies (*n* > 12 per group). (**E**) Axon growth of slices derived from *Il4r*$^{-/-}$ mice in the presence or absence of Th2 cells (*n* = 12–18 per condition). (**F**) Axon ingrowth coculture model of the entorhinal cortex and hippocampus in vitro (33). Entorhinal cortex (EnC) explants of mice, which express EGFP under control of the β-actin promoter with wild-type hippocampus (HC). The perforant path (PP) fibers originating from EGFP$^+$ EC slices reinnervated the dentate gyrus (DG). CA, cornu ammonis. Scale bars: 300 μm (top); 15 μm (bottom left); 3 μm (bottom right). (**G**) Quantification of the EGFP$^+$ area in the hippocampus in the presence of recombinant IL-4 (500 ng/ml) (*n* = 14–15 per condition). (**H**) qRT-PCR of primary neurons and Th2 cells. NTC, no template control. (**I**) IL-4Rα immunofluorescent staining of cultured neurons. Scale bar: 10 μm. (**J**) Axon density from slices obtained from *Camk2g-Cre Il4r*$^{fl/fl}$ mice incubated with Th2 cells (*n* = 28–32 per condition). (**B**–**E**, **H**, and **J**) *P < 0.05, **P < 0.01, 1-way ANOVA with Bonferroni's post-test. (**G**) *P < 0.05, 2-tailed Student's *t* test. Error bars represent SEM.

undergone rigorous double-blind randomized trials or have failed in these trials (39–41). Treatment with IL-4, therefore, is an especially promising target due to its ability to control both neuroprotection and functional regrowth in the injured CNS, where there are so few viable treatment options.

Methods

Animals. C57BL/6, *Il4*$^{-/-}$, *Rag1*$^{-/-}$, *Myd88*$^{-/-}$, MHCII KO, C57BL/6-*Ubc*^{GFP}, and C57BL/6-β-actin-*GFP* strains of mice were purchased from The Jackson Laboratory; OTII/*Rag1*$^{-/-}$ mice were purchased from Taconic. KN2 mice were a gift from M. Mohrs (The Trudeau Institute, Saranac Lake, New York, USA). B10.PL and BALB/c mice were purchased from Charles River. IL-4R mutant mice (Y500F) were a gift from Talal Chatila (Washington University School of Medicine, St. Louis, Missouri, USA), *Il4r*$^{-/-}$ mice were a gift from Nancy Noben Trauth (NIH, Rockville, USA), *Camk2g-Cre Il4r*$^{fl/fl}$ mice were a gift from Frank Brombacher (University of Cape Town, Cape Town, South Africa), and *Camk2g-Cre* mice were a gift from Gunther Schütz (DKFZ, Heidelberg, Germany). All animals were housed in temperature- and humidity-controlled rooms, maintained on a 12-hour light/dark cycle (lights on 7:00 AM), and age matched in each experiment. All strains were kept in identical housing conditions. All procedures complied with regulations of the Institutional Animal Care and Use Committee at University of Virginia or with German guidelines on the use of laboratory animals.

Retrograde labeling of RGCs. Mice were anesthetized, and the skull was exposed and immobilized in a stereotactic device. Holes were drilled in the skull above the superior colliculus (bilaterally 2.9 mm caudal to bregma and 0.5 mm lateral to midline). One μl 4% Fluoro-Gold was injected 2 mm below the meningeal surface at a rate of 0.5 μl/min using a Hamilton syringe and an automatic injector. The dye was allowed to diffuse into the tissue for 1 minute before the syringe was removed. The scalp was then sutured closed, and the mice were allowed to recover on warming pads at 37°C before being returned to their home cages.

Optic nerve injury. Mice were subjected to an optic nerve injury 3 days after stereotactic surgery. Briefly, mice were anesthetized with a 1:1:8 mixture of ketamine/xylazine/saline. An incision was made in

the connective tissue above the sclera. The venous sinus around the optic nerve was retracted to expose the optic nerve, and the nerve was crushed using an N5 self-closing forceps 2 mm behind the globe for 3 seconds. The mice were then allowed to recover at 37°C on a warming pad before returning to their home cages.

Retina excision. Mice were enucleated, and the corneas removed at the corneal limbus. The lens and the underlying vitreous were removed with forceps. The retinas was separated from the sclera and pigment epithelium. Four cuts were made toward the optic disc, and the retina was mounted on nitrocellulose paper and fixed in 4% PFA overnight. Pictures of all 4 quadrants of the retina were taken at equal distances from the optic disc of the retina using an Olympus IX-71 microscope. The pictures were then counted by a blinded observer to determine the number of RGCs per field.

Spinal cord injury. Mice were anesthetized with a 1:1:8 mixture of ketamine/xylazine/saline. A 15-mm midline skin incision was performed over the T6-T13 vertebra, and the connective and muscle tissues were bluntly dissected to expose the lamina. A laminectomy was performed using rongeurs at T9 to expose the dorsal spinal cord. The vertebral column was stabilized with angled clamps attached to the T7 and T12 transverse processes. A calibrated contusion injury (mild or severe) of the spinal cord was induced by an Infinite Horizon Impactor (IH-0400 Impactor Precision Systems and Instrumentation; severe spinal cord injury) or with a modified SPI Correx Tension/Compression Gage (Penn Tool; mild spinal cord injury) at 10 cN for 3 seconds (42). After injury, the muscles and skin were sutured separately. Mice whose actual force varied by greater than 10% of the calibrated force were removed from analysis. The bladders of all mice were expressed twice a day and were tested for neurologic deficits using the Basso mouse scale for locomotion (18). The Basso mouse scale for locomotion was performed by 2 independent investigators, both of whom were blind to the group identity.

Injection of labeled T cells after spinal cord injury. After MACS separation, T cells were washed twice with PBS and were injected into the spinal cord lesion (1 × 10^5 cells in 1 μl per mouse) using a Hamilton micropipette. For tracing T cell migration in the spinal cord, T cells were incubated with 5 μM CFDA-SE (Molecular Probes, C1157) in PBS (1 × 10^7 cells/ml) for 5 minutes.

T cell adoptive transfer. Total lymphocytes were isolated from total lymph nodes of naive mice. The lymph nodes were passed through a 70-μm screen to obtain a single-cell suspension. The CD4$^+$ T cell population was negatively enriched on autoMACS using the CD4$^+$ T Cell Isolation Kit (Miltenyi Biotec) according to the manufacturer's instructions, and 3 × 10^6 CD4$^+$ T cells were injected i.v. into *Rag1*$^{-/-}$ recipients. The T cells were allowed to reconstitute for the indicated times before optic nerve injury was performed. Engraftment was confirmed by flow cytometry.

Bone marrow chimeras. C57BL/6 mice were subjected to split dose irradiation, receiving a 3.5-Gy dose to sensitize the mouse, followed 24 hours later by a lethal 9.5-Gy dose. Two hours after the second dose of irradiation, the mice were injected i.v. with 10^7 bone marrow cells derived from the femurs and tibias of donor mice, as previously described. For head-covered irradiation, heads were covered with lead shields during both doses of irradiation. Briefly, femurs and tibias were removed from mice, and muscles and tendons were cleaned from the bones. Both ends were cut off, and the marrow was flushed out using a 26-gauge needle with PBS containing 1% FBS. Red blood
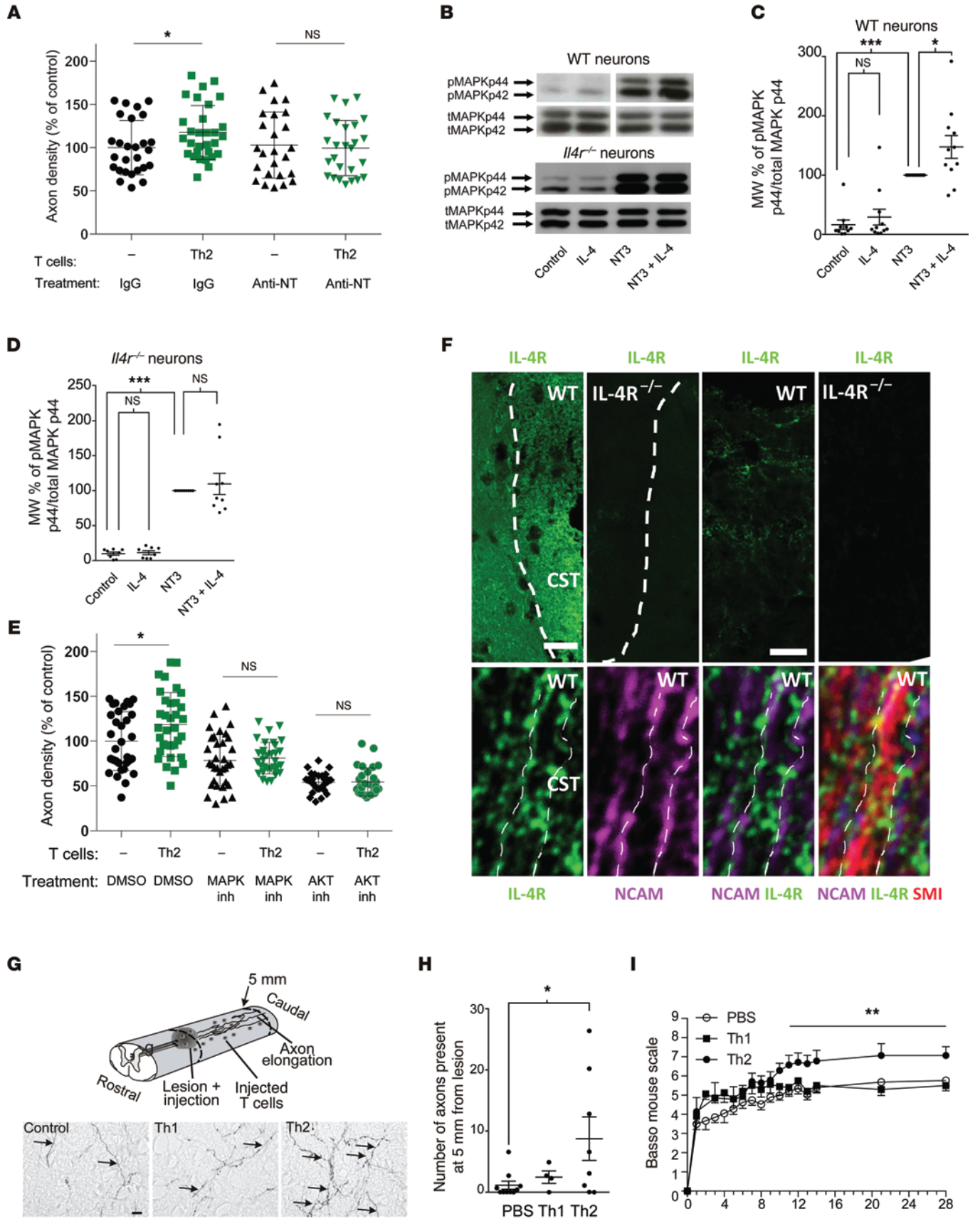
Figure 9. T cell–derived IL-4 potentiates neurotrophin signaling to induce axonal regrowth. (**A**) Combined inhibition of NT-3/NT-4/NGF in cortical cocultures (n = 25–27 per condition). (**B**) Representative blots and quantification of phosphorylated MAPK44 (pMAPK44) and total MAPK44 (tMAPK44) in (**C**) wild-type and (**D**) *Il4r*$^{-/-}$ neuronal cultures that have been treated with IL-4 and/ or NT-3 (n = 11, wild-type; n = 9, *Il4r*$^{-/-}$). (**E**) Inhibition of the MAPK or AKT in cortical cocultures (n = 8–33). (**F**) Immunofluorescence of IL-4R in wild-type spinal cords and IL-4R KO animals. Higher magnification of the IL-4R–positive structures displayed tubular structures indicating a delineation of the axonal membrane (third panel in top row) and no signal in *Il4r*$^{-/-}$ (fourth panel in top row). Immunofluorescence in sections cut along the longitudinal axis of the spinal cord and its long-range axon tracts revealed IL-4R (green signal) located on NCAM-positive membranes (purple signal) of SMI 312-positive axons (red signal; bottom row). Dotted lines indicate axonal membranes. Scale bars: 50 μm (first and second panels, top row); 10 μm (third and fourth panels, top row); 1 μm (bottom row). CST, corticospinal tract. (**G**) Schematic drawing of the injection of Th2 cells after spinal cord injury, with representative photomicrographs. Scale bar: 20 μm. (**H**) Axonal sprouting/regrowth in spinal cord–injured mice injected with Th1 or Th2 T cells (n = 8–10 per condition). (**I**) Locomotion analysis after spinal cord injury by after intralesion injections of skewed CD4$^+$ cells (n = 20, PBS; n = 9, Th2; n = 8 Th1). (**A**, **C**–**E**, and **H**) *P < 0.05, ***P < 0.001, 1-way ANOVA with Bonferroni's post-test. (**I**) **P < 0.01, repeated-measures 2-way ANOVA. Error bars represent SEM.

cells were lysed using ACK lysis buffer, and live cells were counted and resuspended at 10^8 cells/ml. The bone marrow was allowed to engraft for at least 4 weeks before the mice were used for experiments.

Thymus implantation. This procedure was performed as previously described (43). Briefly, thymi were removed from P5 donor pups. Three-week-old mice were anesthetized with a 1:1:8 mixture of ketamine/xylazine/saline. A 15-mm incision was made on skin and peritoneum at the right flank of the recipient mouse, and the kidney was exposed. A scalpel was used to scratch the kidney capsule, and the thymus was implanted below the capsule. The kidney was then returned to the peritoneum, and the peritoneum and skin were sutured closed. The mice were allowed to recover at 37°C on a heating pad before returning to their cages. T cell engraftment was allowed to take place for at least 6 weeks prior to any further manipulation.

In vivo brefeldin A treatment. Two weeks after spinal cord injury, mice were injected i.v. with 300 μg brefeldin A. Five hours after injection, mice were sacrificed, and spinal cords were dissociated with papain and prepared for flow cytometry as described below.

Flow cytometry. For flow cytometric analysis of lymph nodes, the lymph nodes were isolated and passed through a 70-μm strainer in PBS containing 1% BSA and 2 mM EDTA to obtain a single-cell suspension. For flow cytometric analysis of spinal cords, the spinal cords were removed from mice, and the spinal meninges were removed from spinal cords. The spinal cords were minced and then were dissociated for 45 minutes at 37°C in 4 U/ml papain (Worthington Biochemical) with 0.004% DNase added (Sigma-Aldrich). The spinal cords were then triturated to form a single-cell suspension. The cells were spun down and resuspended in 50 μl unlabeled anti-CD16/32 in FACS buffer for 20 minutes at 4°C, and then 50 μl antibody staining cocktail was added for 30 minutes at 4°C, after which the cells were washed and analyzed. The following antibodies were used and are all from eBioscience: CD4-PerCp Cy5.5, TCRβ-APC eFluor780, hCD2-APC, CD45-APC, CD8-eFluor 450, CD19-PE, B220-PE, IL-4–PE, and IFN-γ–APC. The samples were run on cytometers at the UVA Flow Core.

T cell skewing assay. Total lymph nodes were removed from mice, and a single-cell suspension was made by passing the cells through a 70-μm strainer. CD4$^+$ and CD4$^-$ lymphocyte fractions were isolated on autoMACS using magnetic bead separation (Miltenyi Biotec) and incubated in a 2:1 ratio (2 × 10^6 CD4$^-$ cells/ml to 1 × 10^6 CD4$^+$ cells/ml) in the presence or absence of 3 optic nerves/ml in T cell culture media, consisting of RPMI supplemented with 10% FCS, 10 mM HEPES, NEAA, Na-pyruvate, 50 mM 2-mercaptoethanol, L-glutamine, and Penicillin-Streptomycin (Invitrogen). Optic nerves were obtained from either naive uninjured mice or from mice injured 3 days prior to excision. It is clearly stated in the text for each experiment whether the optic nerve was obtained from injured or uninjured donors. In Transwell experiments, nerves were put on top of a 0.4-μm Transwell insert, and in the T cell–only experiments, the CD4$^-$ fraction was omitted. After 72 hours of culture, CD4$^+$ T cells were isolated from total lymph nodes using the CD4$^+$ T Cell Isolation Kit (Miltenyi) according to the manufacturer's instructions. Cells were cultured at 5 × 10^5 cell/ml in RPMI containing 50 μM 2-mercaptoethanol, 100 U/ml IL-2, 10% FBS, 1 μg/ml anti-CD28, NEAA, 10 mM HEPES, sodium pyruvate, and L-glutamate on plates that had been coated with 1 μg/ml anti-CD3 antibody. After 3 days, the cells were moved to a new plate, and the media was supplemented with fresh media lacking anti-CD28 or cytokines. Two days later, the cells were incubated with 10 ng/ml brefeldin A and stimulated with PMA/ionomycin for 5 hours before analysis by flow cytometry. Cells were then stained for extracellular markers, fixed in IC fixation buffer (eBioscience), and stained for intracellular markers in 0.3% saponin.

Primary neuronal cultures. Primary neuronal cells were prepared from E15 BALB/c mouse cortices by enzymatic dissociation using 0.5% trypsin and DNase treatment (0.1 mg/ml) in HBSS, followed by mechanical dissociation by trituration to obtain a single-cell suspension. Cells were seeded on poly-D-lysine–coated cell culture plates directly (96-well plate) or on coated coverslips placed inside the wells of a 24-well plate and cultured at 37°C and 5% CO$_2$ in Neurobasal medium containing 2% B-27, 1% L-glutamine, and 1% penicillin/streptomycin for 2 hours prior to the start of the experiments. All cell culture reagents were from Gibco (Invitrogen). Neurite length from single neuronal cells was analyzed using ImageJ analysis software (NIH) as described previously (44). The length of the longest neurite of 50 single neurons per condition was measured using the following criteria. Neurites innervating other neurons and neurites running out of the picture were excluded from the data, and the length should be longer than the diameter of the cell body. The mean neurite length per condition was determined, and data were expressed as mean ± SEM. Experiments were repeated 4 times (n = 4).

Western blot. Cells were grown for 6 days in neuronal medium, and IL-4 (10 ng/ml) was added 2 hours before the addition of NT-3 (10 ng/ml, Peprotech Inc.) for 5 minutes. Cells were lysed, and protein concentrations were determined by the BCA protein assay (Pierce). Ten μg of each sample were electrophoresed on 10% SDS-PAGE and electrotransferred to PVDF membranes, which were blocked with 2% BSA in TBST for 1 hour at room temperature. Primary anti–phospho-MAPK p42/44 antibodies (1:250, Cell Signaling) were incubated overnight at 4°C. The HRP-linked secondary antibodies were incubated for 1 hour at room temperature (1:5,000), and signals were detected using the ECL Plus System (all Amersham Pharmacia). Membranes were stripped and Western blotting was performed as described above with primary anti-
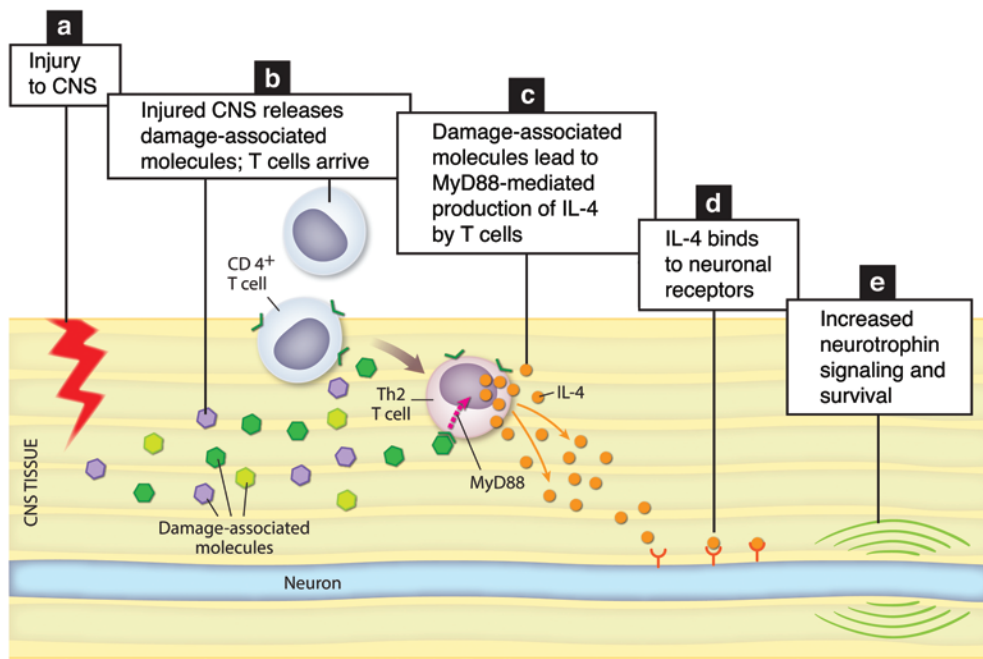
Figure 10. Schematic representation of the proposed molecular events within the injured CNS. (a) Injury to the CNS results in (b) in T cell recruitment to the site of injury and in induction of damage-associated molecular mediators. (c) Damage-associated molecular mediators released from the injured CNS signal on T cells to induce IL-4 expression in MyD88-dependent manner. (d) T cell–derived IL-4 signals through neuronal IL-4R to (e) potentiate neurotrophin signaling and increase neuronal survival.

bodies of the nonphosphorylated protein forms (1:250, Cell Signaling) and HRP-linked anti-rabbit antibody (1:5,000). Analysis was performed with Alpha Imager or ImageJ software. Values were calculated as the percentage of phosphorylated protein to total protein. Values were normalized to NT-3 (=100%).

qRT-PCR. RNA was isolated with the Bioline Isolate RNA Kit, according to the manufacturer's instructions. cDNA was synthesized using the Applied Biosystems High-Capacity Reverse Transcription Kit according to the manufacturer's instructions, and the resulting cDNA was analyzed on a CFX384 qPCR system from Bio-Rad using a TaqMan primer for *Gata3*, with *Gapdh* as an internal loading control (Applied Biosystems).

Generation of ConA-activated T cells. Briefly, we prepared cultures of mixed lymphocytes from spleens and lymph nodes (4 × 10⁶ cells/ml) and stimulated them with 1 μg/ml ConA. To generate Th1 T cells, we added 1–50 ng/ml recombinant mouse IL-12 (R & D Systems) and 1 μg/ml anti-mouse IL-4 (clone 11B11, BD Pharmingen). To generate Th2 cells, 4 ng/ml recombinant mouse IL-4 (BD Pharmingen) and 1 μg/ml anti-mouse IL-12 (BD Pharmingen) were added. Between days 7 and 9, the T cells were restimulated with ConA, using irradiated splenocytes and thymocytes functioning as antigen-presenting cells. This was carried out in the presence of IL-12 and anti–IL-4 for the expansion of Th1 cells or IL-4 and anti–IL-12 for the expansion of Th2 cells. After restimulation, CD4⁺ T cells were prepared by MACS (Miltenyi Biotec).

Cocultures of organotypic cortex explants and T helper cells and EC with hippocampal slices. Briefly, collagen type I from rat tail (Sigma-Aldrich) was dissolved in 0.1 M acetic acid at a final concentration of 2 mg/ml. Of the collagen solution, 1 ml was mixed with 50 μl DMEM medium (Gibco) and neutralized (pH 7.4) with reconstitution buffer (2.2% sodium bicarbonate in 0.8 M NaOH solution). Organotypic slice cultures were prepared as follows. Briefly, the entorhinal cortex was dissected from P2–P3 murine brains and cut into 350-μm-thick slices using a tissue chopper (Technical Products International). Collagen drops (30 μl) containing homogenously distributed T cells were placed

on a glass slide and each slice was placed directly next to the explants derived from mice of the same strain in a collagen matrix (1.2 × 10⁵ cells per drop, 1 drop = 30 μl collagen). Consecutive covering of the T cell drop and the explant with another drop of collagen (30 μl) ensured a standardized distance from the edge of the T cell drop. The sterile cultivation medium contained 25% HBSS, 25% heat-inactivated normal horse serum, 8 g/l MEM HEPES, 4 mM L-glutamine, 4 mg/l insulin, 0.58% bicarbonate solution (Gibco), 1.2% Glucose-20 (Braun), 1% penicillin-streptomycin solution (×100), 0.8 mg/l vitamin C, and 5 mM Trisbase (Sigma-Aldrich) at pH 7.35. The collagen cocultures were incubated at 37°C in a humidified atmosphere with 5% CO₂. After 48 hours in vitro, the collagen cocultures were analyzed microscopically.

Cocultures of EC and hippocampal slices derived from β-actin-*GFP* mice (EC) and wild-type mice (hippocampus) were obtained and prepared as described elsewhere (33). Recombinant IL-4 was directly applied to the culture medium.

Measurement of axonal growth from cortical slices. To evaluate axonal outgrowth from the explants, we used a highly reliable evaluation procedure described previously (45), using image analysis software (ImageJ) to quantify axonal density after 2 days in culture. Neurite outgrowth was photodocumented at a total magnification of ×100, using a ×10 Olympus LCPLANFL objective (Olympus IX70). To determine axonal density, image processing was based on the Sobel algorithm, which performs a 2D spatial gradient measurement in a microphotograph and so emphasizes regions of high spatial density that correspond to axons in the area investigated. To determine the axonal density, the mean intensity was calculated in a standardized area in a microphotograph of every single cortical slice. Values were normalized to the mean of the control (= 100%).

Inhibitors. The following blocking antibodies were mixed into the collagen and compared with the corresponding control antibodies in the same concentration: rabbit anti-mouse NGF (2 μg/ml, IBT), rabbit anti–NT-4 (25 μg/ml, Millipore), chicken anti-human NT-3 (25 μg/ml, Promega), chicken IgY (25 μg/ml, Promega), and rabbit IgG (27 μg/ml, Sigma-Aldrich).

Image analysis of EC-hippocampal cocultures. For the analysis of EGFP⁺ axons in the EGFP/wild-type coculture model, the average intensity in a standardized area (1.1% deviation in area size) was compared using MetaMorph Image Software (Visitron Systems).

Immunofluorescent staining. Immunofluorescent staining was performed using standard protocols. Briefly, after administrating an overdose of anesthetics, mice were transcardially perfused with 4% PFA. The spinal cord was prepared, post-fixed for 1 hour in 4% PFA, and cut on a vibratome, and antigen retrieval (EnVision Flex, DAKO) was performed using standard procedures. Spinal cord sections were subsequently treated with 5% NGS and 0.1% Triton for 1 hour and were incubated with monoclonal antibody against the IL-4Rα chain (BD Biosciences) for 48 hours at 4°C, which was visualized by a secondary Alexa Fluor 488–labeled antibody (Invitrogen, Life Technologies GmbH). Sections were subsequently incubated with a monoclonal antibody against SMI 312 (Covance) for 3 hours at room temperature and visualized by a secondary Alexa Fluor 568–labeled antibody. Images were taken using a Leica SP8 confocal microscope (Leica). To test for antibody specificity, wild-type and $Il4r^{-/-}$ spinal cord sections were imaged using the same microscope settings.

Statistics. Statistics were performed with GraphPad Prism statistical software (GraphPad Software). Statistical methods used were Student's *t* test (only 2-tailed tests are used throughout), 1-way ANOVA with Bonferroni's post-test, and 2-way ANOVA with Bonferroni's post-test. A *P* value of less than 0.05 was considered significant. The specific test used in each experiment is clearly mentioned in the figure legends.

Study approval. All procedures were approved by and complied with regulations of the Institutional Animal Care and Use Committee at University of Virginia or with German guidelines on the use of laboratory animals.

Address correspondence to: Frauke Zipp, Neurology Department, Focus Program Translational Neuroscience (FTN) and Immunotherapy (FZI), Rhine Main Neuroscience Network (rmn²), Johannes Gutenberg University Medical Center Mainz, Langenbeckstr. 1, 55131 Mainz, Germany. Phone: 0049.6131.17.2510; E-mail: Frauke.zipp@unimedizin-mainz.de. Or to: Jonathan Kipnis, Department of Neuroscience, University of Virginia, 409 Lane Rd., MR4, Charlottesville, Virginia 22908, USA. Phone: 434.982.3858; E-mail: kipnis@virginia.edu.

1. Yoles E, Schwartz M. Degeneration of spared axons following partial white matter lesion: implications for optic nerve neuropathies. *Exp Neurol*. 1998;153(1):1–7.
2. Bettelli E, Baeten D, Jäger A, Sobel RA, Kuchroo VK. Myelin oligodendrocyte glycoprotein-specific T and B cells cooperate to induce a Devic-like disease in mice. *J Clin Invest*. 2006;116(9):2393–2402.
3. Luger D, et al. Either a Th17 or a Th1 effector response can drive autoimmunity: conditions of disease induction affect dominant effector category. *J Exp Med*. 2008;205(4):799–810.
4. Stromnes IM, Cerretti LM, Liggitt D, Harris RA, Goverman JM. Differential regulation of central nervous system autoimmunity by T(H)1 and T(H)17 cells. *Nat Med*. 2008;14(3):337–342.
5. Cayrol R, et al. Activated leukocyte cell adhesion molecule promotes leukocyte trafficking into the central nervous system. *Nat Immunol*. 2008;9(2):137–145.
6. Krishnamoorthy G, et al. Myelin-specific T cells also recognize neuronal autoantigen in a transgenic mouse model of multiple sclerosis. *Nat Med*. 2009;15(6):626–632.
7. Dunn SE, et al. Peroxisome proliferator-activated receptor delta limits the expansion of pathogenic Th cells during central nervous system autoimmunity. *J Exp Med*. 2010;207(8):1599–1608.
8. Popovich PG, Stokes BT, Whitacre CC. Concept of autoimmunity following spinal cord injury: possible roles for T lymphocytes in the traumatized central nervous system. *J Neurosci Res*. 1996;45(4):349–363.
9. Fee D, et al. Activated/effector CD4⁺ T cells exacerbate acute damage in the central nervous system following traumatic injury. *J Neuroimmunol*. 2003;136(1–2):54–66.
10. Moalem G, Leibowitz-Amit R, Yoles E, Mor F, Cohen IR, Schwartz M. Autoimmune T cells protect neurons from secondary degeneration after central nervous system axotomy. *Nat Med*. 1999;5(1):49–55.
11. Hauben E, et al. Passive or active immunization with myelin basic protein promotes recovery from spinal cord contusion. *J Neurosci*. 2000;20(17):6421–6430.
12. Frenkel D, Huang Z, Maron R, Koldzic DN, Moskowitz MA, Weiner HL. Neuroprotection by IL-10-producing MOG CD4⁺ T cells following ischemic stroke. *J Neurol Sci*. 2005;233(1–2):125–132.
13. Kipnis J, Mizrahi T, Hauben E, Shaked I, Shevach E, Schwartz M. Neuroprotective autoimmunity: Naturally occurring CD4(+)CD25(+) regulatory T cells suppress the ability to withstand injury to the central nervous system. *Proc Natl Acad Sci U S A*. 2002;99(24):15620–15625.
14. Jones TB, et al. Passive or active immunization with myelin basic protein impairs neurological function and exacerbates neuropathology after spinal cord injury in rats. *J Neurosci*. 2004;24(15):3752–3761.
15. Archambault AS, Sim J, Gimenez MA, Russell JH. Defining antigen-dependent stages of T cell migration from the blood to the central nervous system parenchyma. *Eur J Immunol*. 2005;35(4):1076–1085.
16. Tikhonova AN, et al. αβ T cell receptors that do not undergo major histocompatibility complex-specific thymic selection possess antibody-like recognition specificities. *Immunity*. 2012;36(1):79–91.
17. Kipnis J, Yoles E, Schori H, Hauben E, Shaked I, Schwartz M. Neuronal survival after CNS insult is determined by a genetically encoded autoimmune response. *J Neurosci*. 2001;21(13):4564–4571.
18. Basso DM, Fisher LC, Anderson AJ, Jakeman LB, McTigue DM, Popovich PG. Basso Mouse Scale for locomotion detects differences in recovery after spinal. *J Neurotrauma*. 2006;23(5):635–659.
19. Takeda S, Rodewald HR, Arakawa H, Bluethmann H, Shimizu T. MHC class II molecules are not required for survival of newly generated CD4⁺ T cells, but affect their long-term life span. *Immunity*. 1996;5(3):217–228.
20. Nešić D, Vukmanović S. MHC class I is required

for peripheral accumulation of CD8+ thymic emigrants. *J Immunol*. 1998;160(8):3705–3712.

21. Derecki NC, et al. Regulation of learning and memory by meningeal immunity: a key role for IL-4. *J Exp Med*. 2010;207(5):1067–1080.

22. Baruch K, et al. CNS-specific immunity at the choroid plexus shifts toward destructive Th2 inflammation in brain aging. *Proc Natl Acad Sci U S A*. 2013;110(6):2264–2269.

23. Blaeser F, et al. Targeted inactivation of the IL-4 receptor alpha chain I4R motif promotes allergic airway inflammation. *J Exp Med*. 2003;198(8):1189–1200.

24. Reichardt LF. Neurotrophin-regulated signalling pathways. *Philos Trans R Soc Lond B Biol Sci*. 2006;361(1473):1545–1564.

25. Falcone M, Bloom BR. A T helper cell 2 (Th2) immune response against non-self antigens modifies the cytokine profile of autoimmune T cells and protects against experimental allergic encephalomyelitis. *J Exp Med*. 1997;185(5):901–907.

26. Zheng W, Flavell RA. The transcription factor GATA-3 is necessary and sufficient for Th2 cytokine gene expression in CD4 T cells. *Cell*. 1997;89(4):587–596.

27. Mohrs K, Wakil AE, Killeen N, Locksley RM, Mohrs M. A two-step process for cytokine production revealed by IL-4 dual-reporter mice. *Immunity*. 2005;23(4):419–429.

28. Oppenheim JJ, Tewary P, de la Rosa G, Yang D. Alarmins initiate host defense. *Adv Exp Med Biol*. 2007;601:185–194.

29. Pasare C, Medzhitov R. Toll-dependent control mechanisms of CD4 T cell activation. *Immunity*. 2004;21(5):733–741.

30. Kawai T, Adachi O, Ogawa T, Takeda K, Akira S. Unresponsiveness of MyD88-deficient mice to endotoxin. *Immunity*. 1999;11(1):115–122.

31. Garlanda C, Dinarello CA, Mantovani A. The interleukin-1 family: back to the future. *Immunity*. 2013;39(6):1003–1018.

32. Woodhams PL, Atkinson DJ. Regeneration of entorhino-dentate projections in organotypic slice cultures: mode of axonal regrowth and effects of growth factors. *Exp Neurol*. 1996;140(1):68–78.

33. Hechler D, Boato F, Nitsch R, Hendrix S. Differential regulation of axon outgrowth and reinnervation by neurotrophin-3 and neurotrophin-4 in the hippocampal formation. *Exp Brain Res*. 2010;205(2):215–221.

34. Prang P, Del Turco D, Kapfhammer JP. Regeneration of entorhinal fibers in mouse slice cultures is age dependent and can be stimulated by NT-4, GDNF, and modulators of G-proteins and protein kinase C. *Exp Neurol*. 2001;169(1):135–147.

35. Sun XJ, et al. Role of IRS-2 in insulin and cytokine signalling. *Nature*. 1995;377(6545):173–177.

36. Zweifel LS, Kuruvilla R, Ginty DD. Functions and mechanisms of retrograde neurotrophin signalling. *Nat Rev Neurosci*. 2005;6(8):615–625.

37. Flugel A, et al. Migratory activity and functional changes of green fluorescent effector cells before and during experimental autoimmune encephalomyelitis. *Immunity*. 2001;14(5):547–560.

38. Hendrix S, Nitsch R. The role of T helper cells in neuroprotection and regeneration. *J Neuroimmunol*. 2007;184(1-2):100–112.

39. Bennett MH, Trytko B, Jonker B. Hyperbaric oxygen therapy for the adjunctive treatment of traumatic brain injury. *Cochrane Database Syst Rev*. 2012;12:CD004609.

40. Ma J, Huang S, Qin S, You C. Progesterone for acute traumatic brain injury. *Cochrane Database Syst Rev*. 2012;10:CD008409.

41. Sydenham E, Roberts I, Alderson P. Hypothermia for traumatic head injury. *Cochrane Database Syst Rev*. 2009;2(2):CD001048.

42. Boato F, et al. Absence of IL-1β positively affects neurological outcome, lesion development and axonal plasticity after spinal cord injury. *J Neuroinflammation*. 2013;10:6.

43. Buch T, et al. MHC class II expression through a hitherto unknown pathway supports T helper cell-dependent immune responses: implications for MHC class II deficiency. *Blood*. 2006;107(4):1434–1444.

44. Slaets H, et al. Oncostatin m reduces lesion size and promotes functional recovery and neurite outgrowth after spinal cord injury. *Mol Neurobiol*. 2014;50(3):1142–1151.

45. Boato F, et al. Interleukin-1 beta and neurotrophin-3 synergistically promote neurite growth in vitro. *J Neuroinflammation*. 2011;8:183.